Modelling of the dynamics of a 40 mm gun and ammunition system during firing

N. Eches[1], D.Cosson[1], Q. Lambert[2,3], A. Langlet[3], J. Renard[3]

1 Nexter Munitions, 7 route de Guerry, 18023 Bourges Cedex, France
2 C.T.A. International. 8 route de Guerry, 18023 Bourges Cedex, France
3 Institut PRISME, UPRES 4229 / Equipe Risques Explosions Structures, Université d'Orléans. 63 avenue de Lattre de Tassigny, 18020 Bourges Cedex, France.,

Summary:

This paper deals with the development of a finite element model of a 40 mm Case Telescoped Ammunition and its associated gun, able to describe the in-bore travel of the projectile during firing. This work is part of a PhD thesis, supervised by CTA International and the PRISME Institute, dedicated to the study of the parameters relevant to the accuracy of the Kinetic Energy Round. In order to conduct efficient parametric studies, they asked Nexter Munitions to take the lead for the finite element simulations of the in-bore travel, which is expected to be one of the most contributing phases of the firing event on the ammunition consistency. Nexter Munitions has set up a gun/ammunition model, applying the principles used for the same kind of work in 120 mm ([1] and [2]). The 40 mm study added some issues such as the progressive rifling of the gun, and the slipping obturator, which reduces the projectile spin rate.

The model is compared to actual firing carried out by CTAI, through the strains measured on strain gages lying on the barrel and on an instrumented penetrator, fitted with an on-board data recorder. The paper focuses on the correlation between the strain gages measurements and the simulation of the exact test configuration. It was necessary to run several configurations, with different contact logic and friction coefficients to match simulation and experiment.

Keywords:

Weapon system, Kinetic Energy Munitions, Measuring techniques

1   Introduction

The efficiency of armour piercing fin stabilised discarding sabot projectiles (APFDS) is primarily linked to their terminal ballistics performances. But other parameters, such as its accuracy and its yaw at impact have also a large influence on the performance. These two parameters magnitude, as well as the survivability of the projectile during the launch phase are greatly affected by the interaction between the projectile and the gun. Nexter Munitions developed a methodology to study the gun and ammunition response in calibre 120 mm during the late nineties ([1], [2]). In 2006, the company CTA International[1] launched a PhD thesis on this subject, based on the 40 mm Case Telescoped Ammunition system, in cooperation with the Bourges laboratory of Institut Prisme. They asked Nexter Munitions to conduct the finite element simulations of the in-bore travel, according to the methodology quoted above. In parallel, they developed, with the electronics lab at Nexter Munitions a protocol to dynamically measure the penetrator strains during the in-bore travel. The results obtained were then compared to the finite element model outputs.

2   What is a Case Telescoped Ammunition?

A traditional medium calibre weapon system uses rounds of ammunition having the propulsion system fitted on the rear half of the projectile. The case, containing the propellant has a larger diameter than the projectile, and the ammunition looks like a bottle. It is loaded in the rear part of the gun barrel, whose diameter is larger than the calibre in order to fit the case. The transition between this large diameter and the main bore diameter (the calibre) is made through several cones. The bore of the barrel is rifled, with a twist, in order to impart to the projectile a spin velocity, which will stabilise it along its trajectory to the target. An obturator attached to the shell seals the volume behind it, where the propulsion gases lie. This obturator is made of soft material in order to allow him to be engraved in the rifling groove, and to be able to transmit the twisting torque to the shell. Before being loaded into the gun, the cartridges are linked together with connectors, which are snapped off the round prior the introduction. This system leads sometimes to weapon jamming.

The 40 mm Case Telescoped Ammunition (CTA) consists of a projectile completely embedded inside the case. Such an ammunition, at identical calibre, yields better terminal performances, and a reduction in bulk volume of 30%. In addition, the loading of the round into the gun chamber is done without connectors, which is more reliable and prevent weapon jamming.

In terms of in-bore behaviour, the main differences with a classical medium calibre system is that the chamber is not part of the barrel, as it is a mobile assembly, rotating around a vertical axis, in order to eject the case remaining from the previous firing and load a fresh round for the next shot. Thus the projectile begins to be accelerated in the chamber, and already has a velocity when it enters the forcing cone and begins the engraving.
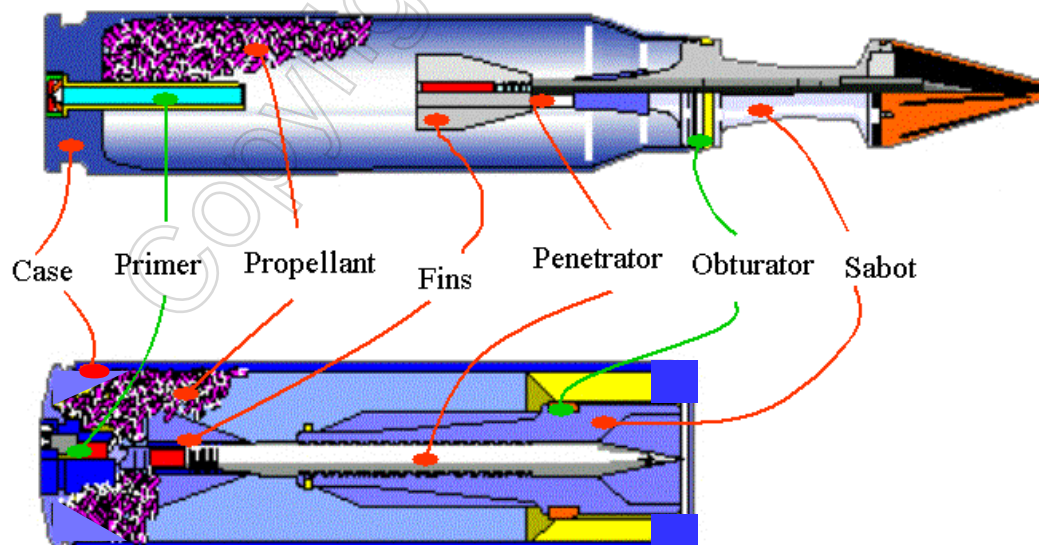

Figure 1: Comparison of traditional Medium Calibre ammunition (above) and 40 mm CTA (below)

---

[1] CTA International is a JV company, jointly owned by BAE SYSTEMS Land Systems UK and NEXTER SYSTEMS FR, dedicated to the development, manufacturing and sale of the 40mm Cased Telescoped Armament System.

3   Model set-up

Between 1998 and 2005, Nexter Munitions (known at that time as Giat Industries) conducted studies to simulate the gun dynamics events (see. Ref. [1] and [2]) through the mean of finite element analysis. This kind of simulation was initiated by Rabern ([3]), who first calculated the interactions between a projectile and a gun barrel, and enhanced by Wilkerson and Hopkins ([4] and [5]), who introduced the complete weapon in the model, Our idea was to go a step further by simulating a closer behaviour or the projectile, thanks to the inclusion of the interactions between the different components of an APFSDS shell, including the grooved interface between the penetrator and the sabots. These works were related to the modelling of a 120 mm smoothbore gun and ammunition system, which is very different of a 40 mm CTA system as shown in the following table:

System	120 mm	40 mm
Barrel	Smooth	Rifled
Chamber	Part of the barrel	Outside the barrel
Recoil system	Hydraulic	Spring

Nevertheless, most of the principles used at that time are still valid, and some features had to be added.

3.1   Model requirements.

This model is intended to be used for parametric studies, whose purpose will be to examine the influence of several ammunition and gun parameters on the exit condition of the projectile (displacements and velocities). So it must be as faithful as possible to the actual weapon system to avoid misleading results coming from wrong modelling hypotheses. Among the requirements we set, the main ones were:
-   exact geometry and interfaces between parts. The weapon includes several parts, some of them sliding against other. The model must simulate as well as possible all the internal interactions of the system, with their clearances and friction.
-   modelling of the interactions between projectile and sabots i.e. slide surface between two sabot petals, and between sabots and penetrator.
-   Penetrator driven by the sabot. In the actual round, the thrust of propulsion gases is transmitted from the sabot to the penetrator by the means of grooves machined along the rod. The model must reproduce this arrangement, with contact between the grooves on the penetrator and the teeth on the sabot.
-   Barrel wall loaded by the propellant gases. When the propellant is ignited, it burns very fast, producing a huge amount of high pressure hot gases. These gases apply their pressure onto the sabot part aft the obturator, the fin and the part of the rod situated between the sabot and the fin. They also apply their pressure onto the barrel wall, on the length situated between the rear end of the gun and the projectile obturator. This surface increases continuously, as the projectile goes forward, uncovering non loaded zones of the tube. The model must be able to simulate the propagation of the barrel wall loading along the projectile displacement.
-   Projectile spin driven by the rifling grooves. In the actual weapon system, the engraved obturator follows the twist of the rifling, and then drives the shell rotation. When a full calibre shell is fired, the band transmits all the torque to the projectile. When an APFSDS is fired, it must not spin too fast, as it is stabilised by fin. In this case, the obturator slips, and only a fraction of the torque is passed to the sabots, because of fiction. The model must be able to simulate this phenomenon.
-   "working" recoil system. The recoil system of the 40 mm CTWS gun is powered by springs, unlike the 120 mm, which uses a hydraulic principle. In that case, a pre-programmed recoil force was input into the simulation. With the spring brake, the force will be computed as a function of the instantaneous recoil.
-   Barrel "straightness". A gun barrel is never perfectly straight. First, the machining process induces off-axis defects, and second, the gravity acting on a cantilever beam such as the gun induces an additional curvature. The shape of the longitudinal axis is of prime importance on projectile in-bore balloting and hence, on the exit conditions. Then, the model has to be able to include straightness defects end gravity droop.

3.2   Geometry and mesh generation.

3.2.1 Generalities

The geometry and mesh were generated with the XYZ True Grid pre-processor. This pre-processor has the advantage of producing hexahedral structured mesh, from an explicit fully parametered command language, which can be used either interactively, in batch mode, or between both modes. All the relevant data of the system were parametered, such as: clearances in the slide surfaces, spring displacement-force curves, projectile dimensions, etc… The different cases of the parametric study are then very easily generated by changing one or several parameters in the batch files, and then run the pre-processor in batch mode, producing a complete LS-Dyna data deck in 2 or 3 minutes.
Several tools were developed, to generate True Grid batch files, as we needed some functionalities that are not directly included in the command language.
The reference system uses the Z-axis along the tube centreline direction, while the X and Y-axis are the horizontal and vertical directions.

3.2.2 Weapon

The weapon is divided into two main components: the barrel and breech assembly, (also known as. the recoil mass), and the cradle assembly. The latter comprises a faithful geometric description of the prismatic cradle, including fixtures for external devices, the body of the recoil system, the trunnions and the bearings between the cradle and the barrel.
As the barrel has 12 grooves, it includes 24 elements in its circumference. Thus each rifling tooth is meshed with one element in width and one element in the thickness. This choice was made to reduce the overall mesh size and to keep an acceptable time step, by avoiding too small element dimensions.
As the gun is rifled, the mesh of the barrel is twisted to follow the progressive rifling angle which means that we have wedge shaped elements at the rear end of the barrel (the rifling angle is 0) and slanted wedge shaped element at the muzzle, where the angle is maximum. The attachment of the muzzle brake is twisted as well, to fit the barrel mesh, allowing to merge these two parts.
The barrel axis must follow the straightness curve of the individual mesh we wish to simulate. To do so, the internal diameter of the tube is mapped on a cylinder whose axis is the straightness curve. This mapping must be performed after the mesh twist, in order to avoid to also twist the centreline and rotate the offsets, which could alter the barrel internal geometry. One can do these operations with the True Grid capability of modifying nodes coordinates, once the part is meshed, with Fortran-like equations. This is straightforward for the twist, as the rifling angle is defined by an analytical function, but for the straightness, as the centreline geometry curve is a discrete (x,y) curve, this capability cannot be used directly. It is necessary, for each row of nodes along the barrel longitudinal axis, to calculate, through linear interpolation, the offset of the centreline, and to translate the nodes situated on this raw by this offset. As the barrel counts about 300 rows of nodes, doing this by hand is very tedious, and can be a source of errors. Instead, a Fortran pre-pre-processor was developed, which generates a batch file containing all the instructions to generate the barrel mesh, including the 300 calls to the mesh editing functions.
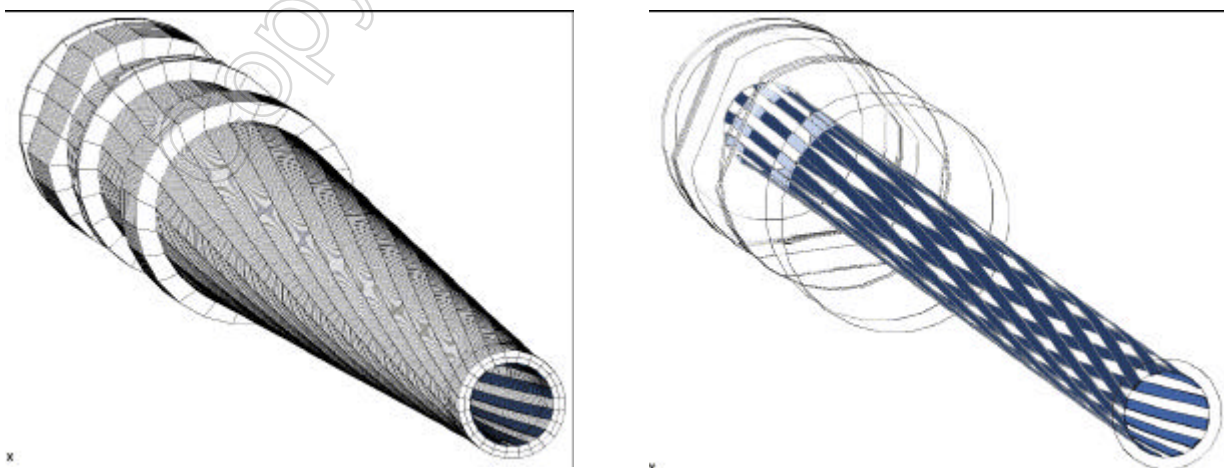

Figure 2: View of the barrel mesh (left) and of the rifling (right).

The recoil system is composed of a rod surrounded by an annular spring, encased in a sleeve, which acts as a piston. When the gun recoils, the sleeve goes backwards, compressing the spring, which generates a counter-effect, decelerating the recoiling mass. The spring stores elastic energy that is used for the setback. This latter phase is not simulated here, as it occurs a long time after the projectile exits the muzzle. We have only to simulate the beginning of the recoil phase. For that, we used beam elements to model the spring. Every node on the perimeter of the piston has a beam attached on it, whose other end is welded on a plate attached to the cradle. The stiffness of each beam element is 1/24 of the spring stiffness.
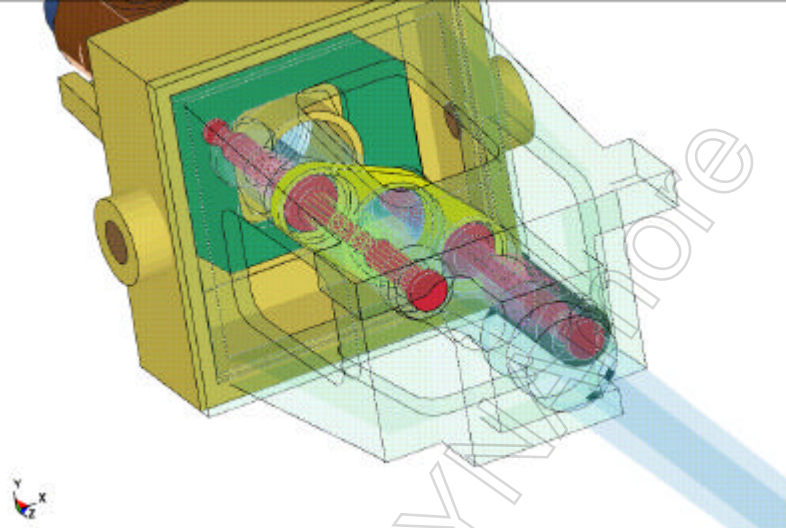

Figure 3: Recoil system model. The rods are red and the sleeves are green with transparency. The yellow part links the sleeves to the barrel, while the green plate is attached to the cradle.

3.2.3 Ammunition

As requested, we have to model the projectile as "really" as possible. Thus, the penetrator-sabot interface is meshed in a realistic way, including the grooves actually present on both the rod and the sabot. Then, the rod and the sabot petals interact through a sliding surface. The propulsion effort is thus transmitted from the sabot to the rod in the most possibly realistic way. Thanks to this methodology, we can take into account the clearance between the penetrator and the sabot assembly, the radial degree of freedom of the sabot in the gun tube, and also we prevent an over-stiffening of the projectile, resulting from the welding of the penetrator to the sabot.

Nevertheless, in order to avoid to deal with too many elements, the actual number of grooves is divided by two, and the geometry of the modelled tooth is such as the slopes and diameters are kept, as well as the total shear surface at pitch radius. The groove simplification is shown on the figure below.
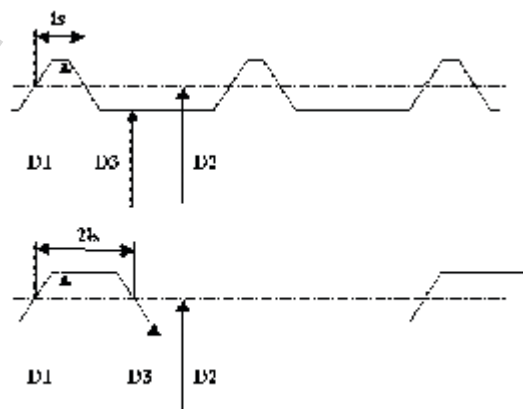

Figure 4: simplification of the rod-sabot interface. Above: actual geometry. Below: model

The fin and the windshield-tip assemblies are modelled as equivalent masses and inertia, still in a seek of simplification.

The obturator had to be adapted to the simulation. The problem comes from the fact that the engraving process very severely distorts the material of the obturator. This process is difficult to simulate, and requires very fine zoning ([6]), which is not adapted to our calculation, because of the rather long duration of the total in-bore travel (? 5 milliseconds). So, the band is meshed "pre-rifled", with grooves in front of the corresponding tooth of the barrel. This is an unavoidable trade-off, but it is not expected to lead to significant errors, as the obturator material for the APFSDS is very soft (thermo-plastic polymer), and does not shows high mechanical properties.

On the contrary to 120 mm, where the case is made of combustible material and has no strength, in the 40 mm CTA, the case is made of steel, and is clamped to the ends of the cartridge. Then it should be taken into account in the simulation. Instead of adding weight to the model with numerous shell elements, the case was represented by a set of 24 springs, whose resultant stiffness is equivalent to its longitudinal stiffness. The lateral behaviour of the cartridge is considered as being of second order and is not included in the simulation.
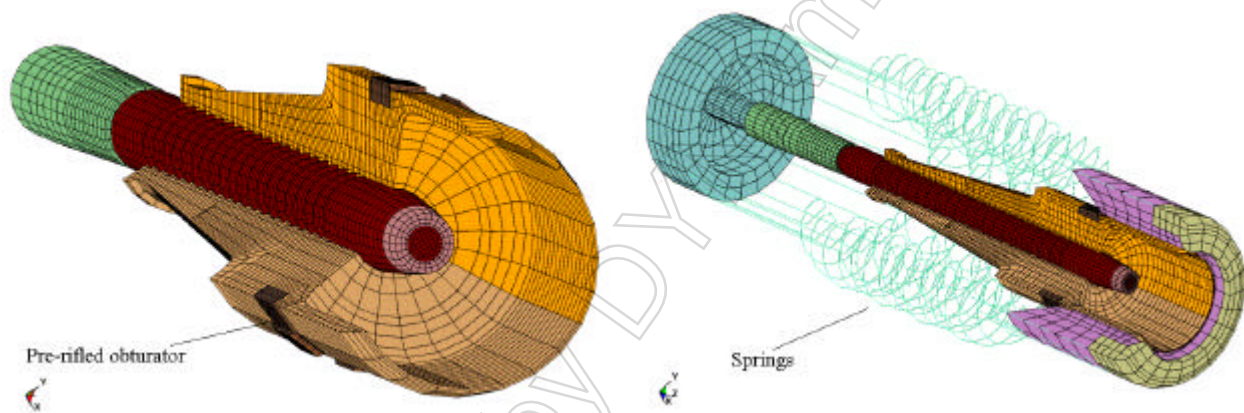

Figure 5: Cut-away Views of the projectile mesh (left) and of the complete round (right) showing the pre-rifled obturator and the springs simulating the case.

3.2.4 Contacts

The model contains numerous sliding surfaces, to manage all the contacts occurring during the firing event as realistically as possible.
A slide surface is set between the barrel and the cradle to allow the recoil.
The projectile-barrel inner wall interface is managed by slide surfaces between the obturator and the tube, and the bore rider and the gun. Slide surfaces are also set between the petals of the sabot, and as we said formerly, between the petals and the grooves of the penetrator.
The last interface lies between the obturator and the bulkhead of the sabot. The actual configuration is very close of a sliding contact with voids, as the obturator is moulded on the bulkhead and can slip tangentially as explained in 3.1. Unfortunately, the geometry of the meshed interface is not a perfect cylinder, but a 24-sided polyhedron. The edges between the faces of the polyhedron prevent the obturator to slip realistically. Then, we chose to tie it on the sabot, and to adapt the rifling angle to lower the torque transmitted to the projectile. Experimental results tell that the exit spin rate for the 40 mm APFSD is about a quarter of the theoretical spin generated by the rifling. Then the twist in the barrel mesh was adapted in order to impart to the projectile the experimental spin rate.

3.2.5 Boundary conditions

Only one boundary condition is applied to the model. It simulates the attachment of the gun to the mounting (armoured vehicle or test rig) and uses translationnal restraints in the three directions of the trunnions pins, while the X-axis rotation is still permitted. The rigid rotation of the whole structure along the trunnions X-axis is prevented by translation restraint on the bushes at the front end of the cradle.
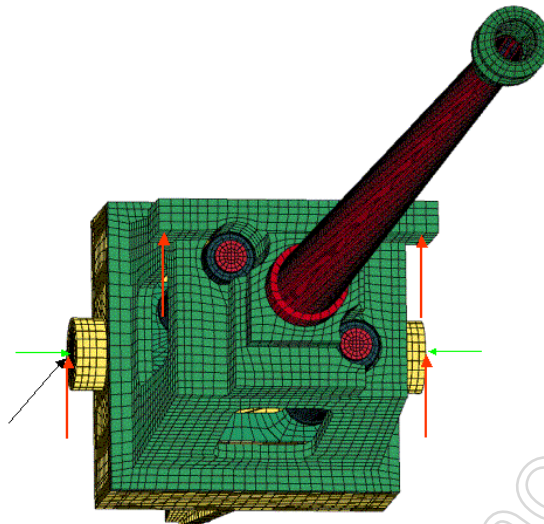
Figure 6: Boundary conditions on the weapon

3.2.6 Loads

The main load applied on the system is the pressure generated by the combustion of the propellant. According to the location where this pressure is applied, the load curves vary. This is due to the fact that a pressure gradient lies along the barrel, between the breech and the projectile. The breech pressure, which we can consider as uniformly applied on the chamber walls, is given by either a lumped parameter internal ballistics code or by pressure gauge measurements. The base pressure, which is applied on the projectile is calculated from the breech pressure thanks to the Piobert correction, and then adjusted in such a way that the muzzle velocity resulting from the acceleration matches the expected muzzle velocity, which yields the axial acceleration by time differentiation, giving directly the pressure.

In reality, the barrel wall is loaded by the pressure of propulsion gases lying between the breech and the projectile. As it proceeds to the muzzle, it uncovers a portion of the barrel wall, which is instantaneously loaded by the gases filling the uncovered volume. Setting a FSI simulation, including the propellant gases was too complicated for the purpose of the study. So we chose to use a weak coupling, i.e. we pre-calculated the times the projectile uncovers a given row of elements of the tube, and defined a specific load curve for this row of elements, starting at 0 MPa when the obturator passes the lower bound of the row of elements and reaching the base pressure when the projectile passes the upper bound of the row. The pressure is then calculated using the linear gradient between breech and projectile hypothesis.

The Fortran code used to generate the barrel mesh includes also the instructions to apply the 300 curves on the suitable rows of barrel elements. This program also includes the definition of all the curves, including the calculation of the projectile passing times in front of the elements. The figure 7 displays the breech and base pressures. The breech pressure is applied on the chamber walls, and on the base and the front part of the cartridge case. This pressure drives the breech deformation and the recoiling mass longitudinal movement. The base pressure, as explained above, loads the projectile from the tail to the bulkhead. Fig. 8 shows four other curves, in red/orange colours, which are some selected examples of the pressure curves applied on the barrel wall. These curves start at 0 MPa, then climb suddenly to the instantaneous base pressure applied on the projectile at the passing time and at the location of the row, and then evolves as a combination of the breech and base pressure, weighted by the projectile location. On the rear end of the tube, this curve is very close to the breech pressure, while on the muzzle side, it is closer to the base pressure. The whole model contains about 300 curves of this type

As the projectile accelerates, a pressure is created in the front cup, as a result of the inertia of the air in front of it. The magnitude of this pressure is estimated by an empirical formula, and reaches about 3 MPa when the shell exits the muzzle. This pressure participates to the sabot separation, as it supplies a lift force that tends to push the sabots outwards.

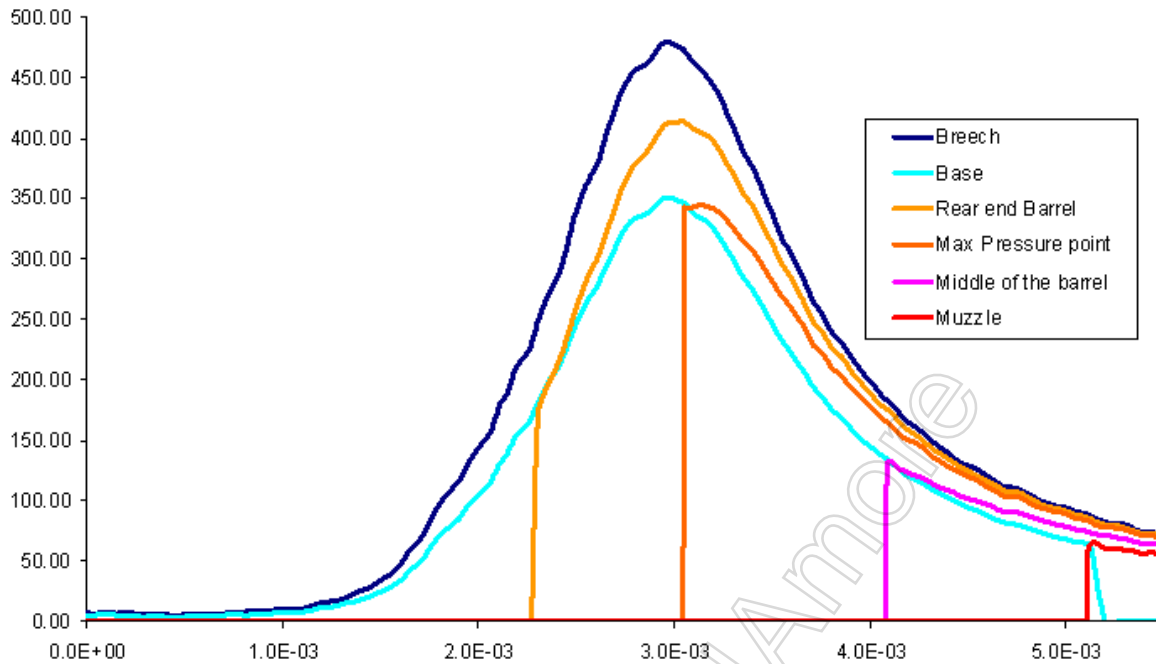A constant gravity is applied on the whole structure for the whole calculation

Figure 7: Pressure curves used for the simulation. Times in seconds, pressures in MPa.

3.2.7 Materials

All the materials constituting the weapon are considered elastic.

The fins and windshield simulants are also modelled with elastic material, while the sabot, the projectile and the obturator follow the elastic-plastic material model n° 24. As, despite the pre-rifling and the lower rifling angle, the obturator experiences very severe deformations on the face in contact with the rifling grooves flanks, its material has a failure strain of 3, in order to allow erosion.

3.3   Simulation sequence

The simulation begins by a static implicit run, whose purpose is to calculate the structure response to gravity. This allows to set the correct barrel droop, to position the projectile in the cartridge, as it is meshed in a theoretical location, which may different of the actual one, which is a function of the deformation of the weapon.

This implicit initialisation is then followed by two dynamic runs. The first one is to determine the exact projectile kinematics. It is necessary because of the weak coupling between the barrel loading and the projectile location. If those two phenomena are not well synchronized, the barrel dilatation will not be in phase with the projectile location, and the results will not be physical. Then, after the first run, the projectile and recoiling mass axial displacements curves are obtained, which will give the exact shell position relatively to the barrel as a function of time, which will used in the Fortran pre-processing code to recalculate the passing times for each raw of elements and hence the barrel wall load curves. On the same time, the exact muzzle time and muzzle velocity are determined, which are used to decrease the base pressure when the projectile leaves the weapon. In the absence of precise data, we guessed that the baser pressure begins to be negligible when the bulkhead rear face leaves the muzzle brake.

It allows also to calculate the time when the obturator will be discarded from the simulation to allow the sabot separation.

The altered data are input into the LS-Dyna deck, and the second explicit run is launched, which yields the final results. The three runs use the double precision version of LS-Dyna.

As the purpose of this model is to lead parametric studies, an other Fortran program has been developed to automatically post-process the results, which give all the information expected by CTAI. As the rigid displacement is in meters, and the local displacement gradients are in tenths of microns, the ". matsum" and ". nodout" files are not accurate enough. Then the program reads the ". d3thdt" family of files instead, where the data are on double precision format. The program presents the results under a summarized form, which makes the comparison between several cases easier.

4   Experimental study

Before entering a comprehensive parametric study, the calibration of the model is requested. To do so, CTAI conducted an experimental study to get results to be compared with the simulation.

For that, the tube was instrumented with strain gages, giving the barrel expansion. Those data were used to determine the projectile kinematics. This kind of instrumentation is commonly used in gun dynamics studies, but it does not yield much of information about the projectile behaviour, which is the focus of the thesis. Then, a projectile instrumentation protocol had been defined, to solve this problem. The principle is to implement strain gauges, set up in Wheatstone bridge in grooves machined on the rod. The bridge measures the half difference of elongation between two opposed gauges. Four pairs of gauges were implemented on the rod, divided in two sets of two pairs.
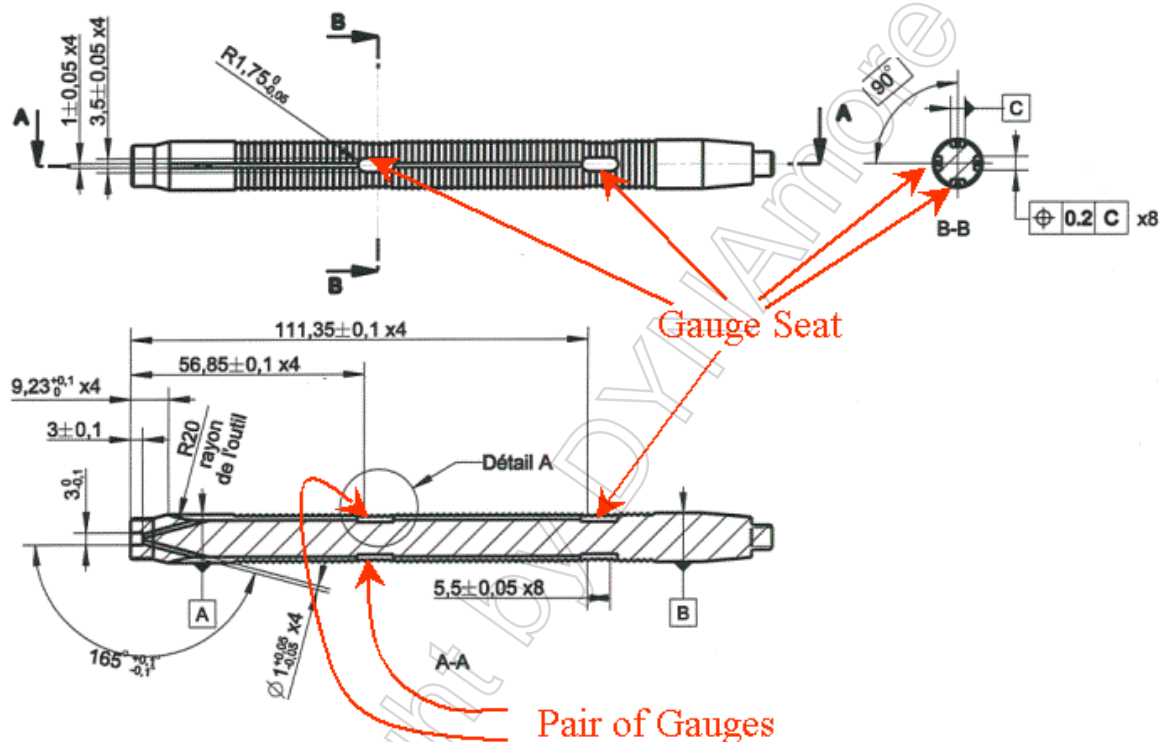

Figure 8: Location of gauges on the penetrator

The grooves contain the gauges and the wires, which go inside a data recorder device, embedded in a 31 mm outer diameter flare mounted in place of the fins. This data recorder has been developed by Nexter munitions and has been proven to survive very high accelerations, as it has been successfully fired in 25 mm (about 100,000 G's) and in anti-bunker penetrator fuses, where it survived the penetration of thick reinforced concrete slabs, while keeping the stored data safe.

The device is completely autonomous, with its on-board power supply. It is switched on prior the loading of the ammunition is the chamber. Once the system is initialised, it lies in idle mode, waiting for the firing. A shock sensor is used to determine that the ignition occurred. Two kinds of triggering were used:

- Simple trig: when the device detects the ignition, it begins to record the signals coming from the gauges. The record stops automatically after 87 ms, which corresponds to the memory capacity, in this configuration.
- Pre-Trig: once the system is initialised, it records continuously the signal coming from the gauges, overlaying previously recorded data when the memory capacity is exceeded. Once the ignition is detected, the system write-protects data from 10% of the memory capacity before the ignition to 90% of the capacity after the ignition. This pre-trig mode has the interest of recording the whole event, while the simple trigs only records after the detection of ignition, which occurs later than the actual beginning of the firing.

The round used to calibrate the model used the pre-trig mode.

Several rounds of ammunition were shot, with different propellants charges, leading to different accelerations and muzzle velocities. The projectiles were fired into a rag box, in order to "gently" decelerate them and to recover the flare in a condition good enough to get the recorded data.
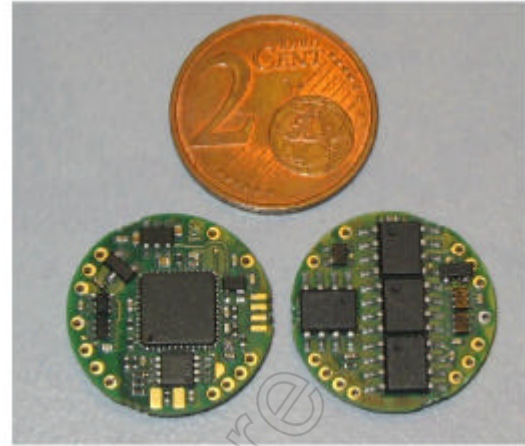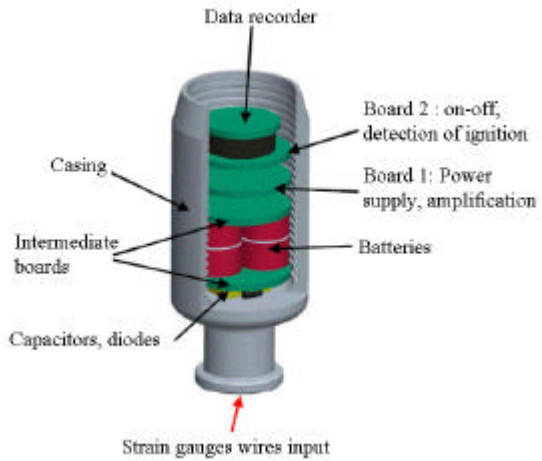
Figure 9: data recorder assembly (left), data recorder board heads and tails (right)

The following figures show the instrumented ammunition

Figure 10: Instrumented ammunition. Strain gauge implemented on the rod (left), complete round with flare (right)

The shot n°6 which yielded the cleaner signal was selected to be compared with simulation. Its muzzle velocity was 1319 m/s (standard muzzle velocity is 1450 ms), with a maximum acceleration of about 80,000 G's. The front pairs of gauges gave the following signals:
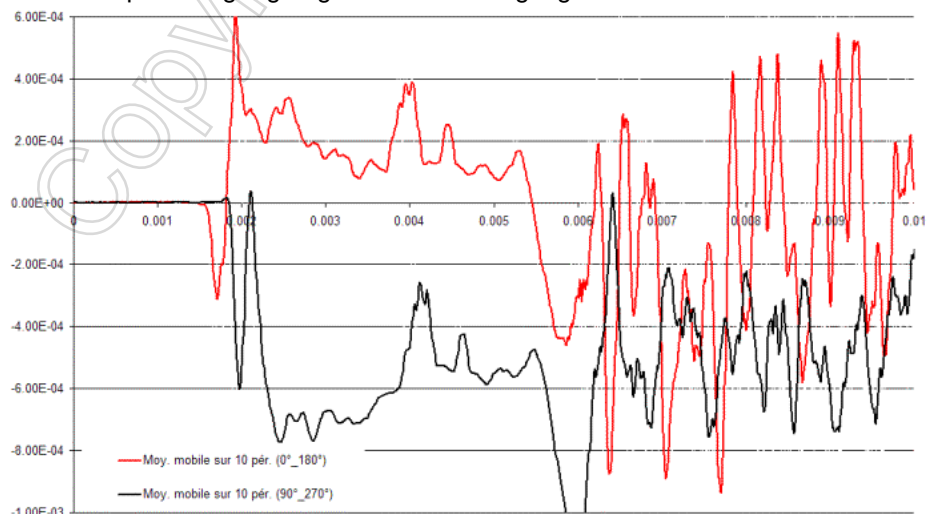

Figure 11: strain gauges (front pairs) signals. Strains in m/m, times in s

The two pairs of gauges are referenced as (0°-180°) and (90°- 270°) regarding their initial position in the gun. As one can see, the two signals are relatively similar, excepting the beginning of the firing. The muzzle time is about 5.46 ms. The end of the two curves are nearly parallel, and show some residual strains (the average of the oscillations after 5.2 ms is not equal to 0). This is surprising because the penetrator, at this low pressure, is not expected to yield.

5   Simulation of the trial.

In order to simulate the test, the model has been updated. The grooves were added to the penetrator, the fin was replaced by a flare, filled with a material whose density was adjusted to give the actual weight. The breech pressure curve was taken from the pressure gauges measurements, and all the other pressure curves were updated, using the methodology described in 3-2-6. The barrel was mapped around the actual straightness curves, given below.
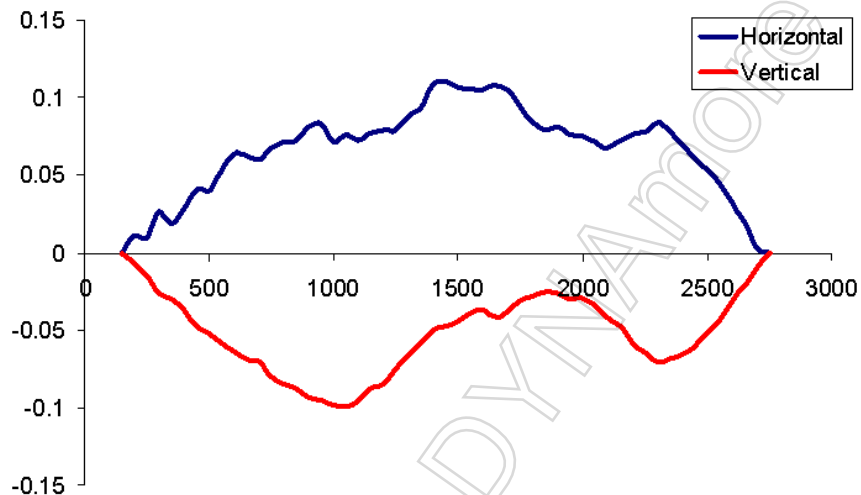

Figure 12 : Barrel straightness curves (offset (in mm) as a function of distance from the rear end (mm))

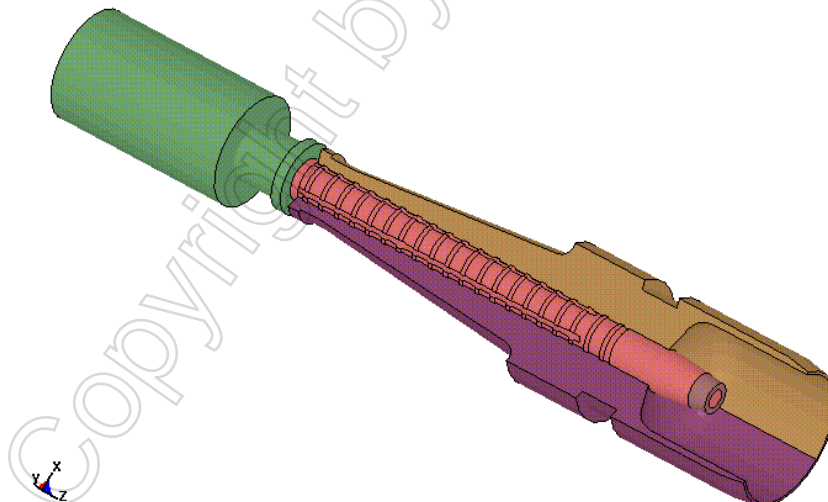The following figure shows the altered projectile The grooves are one element wide.

Figure 13 : modified projectile, simulating the experiment.

The strain gauges are represented by node sets, which are saved in d3thdt. Each set, corresponding to an individual gauge, includes four nodes, being the corners of a rectangle made of two elements outer faces lying around the gauge middle point. The elongation is determined as the averaged displacement difference between the upper and the lower bound of the node set. The post-processing program calculates then the average elongation between two opposite gauges, giving the axial strain of the rod, and the half difference between the two opposite gauges, which can be compared to the experimental measurement. This figure is characteristic of the flexural behaviour of the projectile.

About 50 different simulations were performed, including variation of the initial sabot position (one symmetry plane below the penetrator, or above the penetrator (actual experimental configuration)) and contact logic definition and parameters.
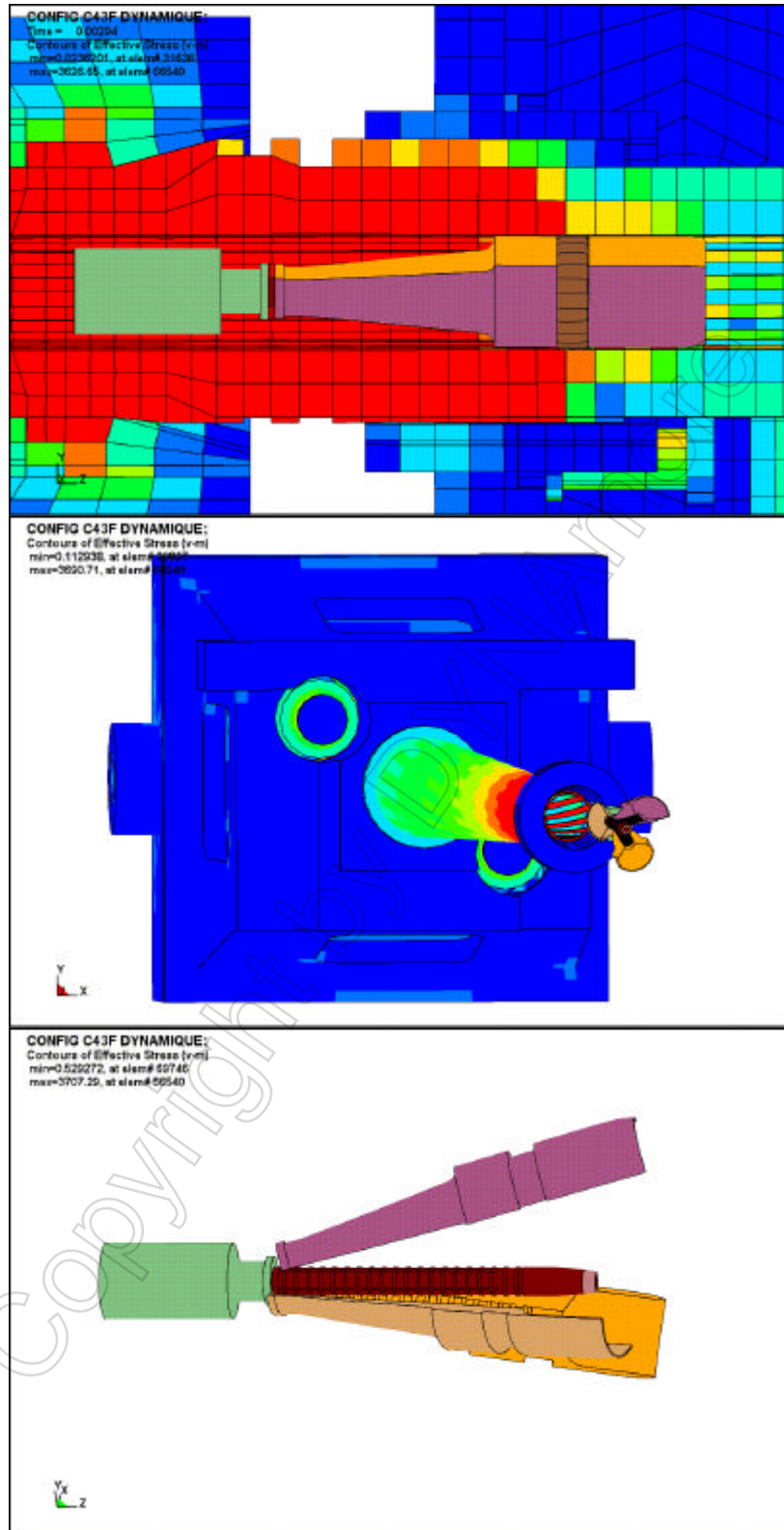
Figure 14 : Views of different stages of the simulation. Top : Introduction of the projectile into the barrel (the weapon is cut out) von Mises stresses on the barrel, showing the wall loading behind the projectile. Middle : von Mises stresses in the weapon at the time of exit. One can see the beginning of sabot separation. Bottom : Sabot separation, one millisecond later.

The study showed that despite the fact the projectile spins during its in-bore travel, the sabot position influences the flexural behaviour of the rod. With the symmetry plane below the penetrator, it was impossible to find curves that we could fit with the test results. With the sabot symmetry plane above the penetrator, the results were better. As an example, here is one case where the correlation between experiment and simulation is very good.
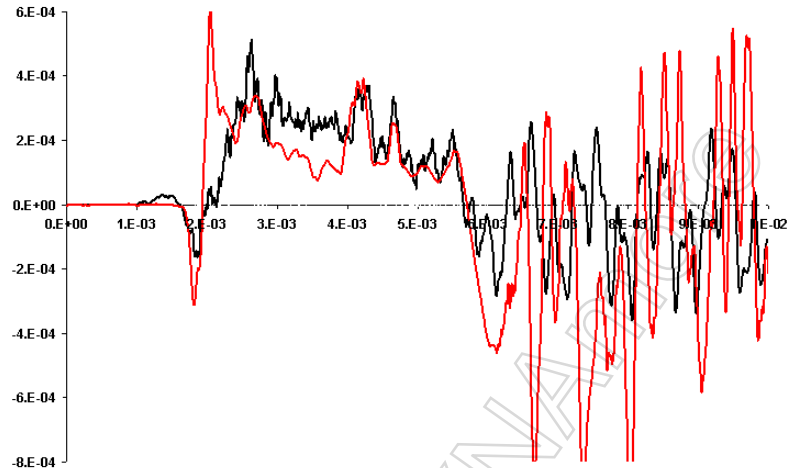

Figure 15 : Comparison between simulation(black) and experiment (red). Strains in m/m, times in s

Unfortunately, the black curve, being the simulation result, corresponds to gauge pair (90°-270°) and the experimental curve, in red, to the other gauge pair. Nevertheless, one can see that the global shape of the curve is correct, with several peaks between 3 and 6 milliseconds which are perfectly captured. The model does not see the first oscillation, which is, according to the time, related to the introduction of the projectile in the barrel, when it leaves the chamber. It is probably due to the initial conditions, such as the chamber misalignment with the barrel axis, or the initial position of the projectile inside the case. It is also possible that the pressure field may not be perfectly axi-symmetric in the beginning of the firing, which may induce penetrator flexions in the earlier times of the event. The contact logics used for this case were as follows :
- Between sabot petals :   surface-to-surface, by parts, no friction
- Between penetrator and sabot :   surface-to-surface, by segments sets, static friction of 0.1

The other pair signal was completely different of the experimental curves. So other contact logic were tested. The modification of the friction coefficient between sabot and penetrator and the introduction of friction between the sabot petals allowed to rotate the rod response of 90°, and to have a correlation (simulation/test) between the same pairs of gauges

Figures 15 and 16 show the examples of configuration 30 and 47.

The configuration are as follows :
- Config 30 :
  - Between sabot petals :   surface-to-surface, by parts, no friction
  - Between penetrator and sabot :   surface-to-surface, by segments sets, static friction of 0.05
- Config 47 :
  - Between sabot petals :   surface-to-surface, by parts, static friction of 0.1
  - Between penetrator and sabot :   surface-to-surface, by parts, static friction of 0.05

As one can see, no configuration captures the first oscillation. In fact, in none of the 50 cases we ran we could see this first oscillation. So we think that this phenomenon is linked to some physical aspect we did not include in our model.

Despite this fact, we can see that according to the contact parameters, we can get rather good correlation between experiment as most of the significant bumps of the curve between –3 ms and the muzzle time are found. The magnitude is not correct for the (90°-270°) pair, but as we told above, it looks like the experimental curve might have shifted, as the residual strains should average to 0.
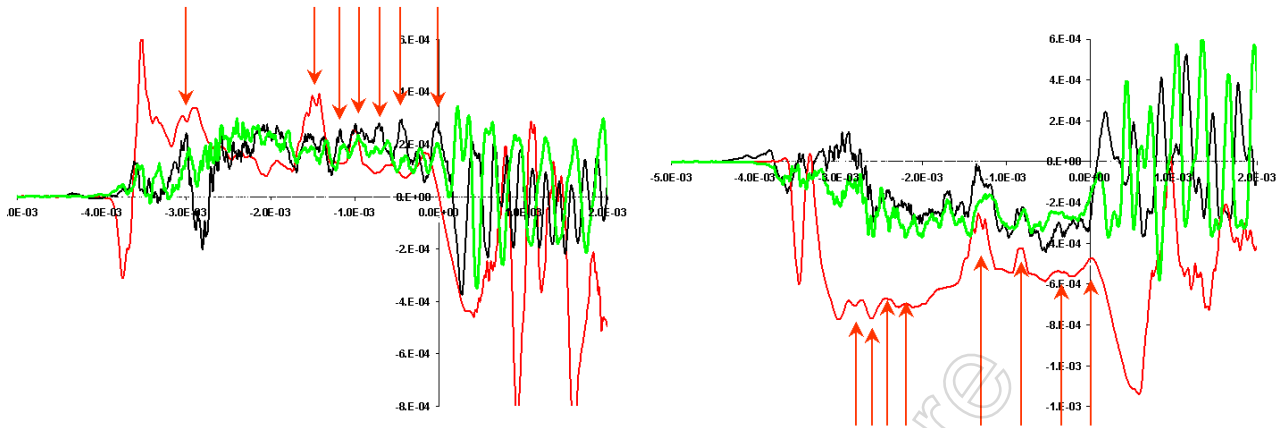
Figure 16 : Comparison between experience (red), config 30 (black) and 47 (green). Left : pair 0-180, right : pair 90-270. Time = 0 is muzzle exit time. Strains in m/m, times in s.

The examination of all the configurations curves led to choose the case 47 contact parameters to go on the parametric studies. Some works are still going on to understand the reason of the apparently odd offset on the gauge pairs (90°-270°) We must stay careful and not conclude too early as we had a single usable test result. Such a model, which simulates a generic configuration should be compared to a collection of tests of the same configuration, which may all differs by several details that are not included in the model, such as initial conditions, pressure fields dissymmetry, CoG offsets.etc….

6   Conclusion

The understanding of complex phenomena like the interactions between a rifled gun and a saboted ammunition is dependant of the modelling capabilities of the design offices. This study shows that Nexter's know-how allows to address this kind of problems. Nevertheless, the best simulation work is senseless without advanced measurement technologies that allow to set a reliable experimental database, that the simulation expert can use to validate his results. The example of the sensitivity of the projectile strains to contact parameters illustrates this issue.
Once the simulation of the test is considered valid, then the power of tools like LS-Dyna, increased by in-house derived tools is very efficient to conduct parametric studies

7   Literature

[1] Eches N. Paugain N., Doffémont C. : In bore behavior of Large Caliber Armour Piercing Fin Stabilized Discarding Sabot projectiles, 3rd European LS-Dyna Conference, 2001

[2] Eches N. Paugain N., Doffémont C. : In bore behavior of Large Caliber Armour Piercing Fin Stabilized Discarding Sabot projectiles, 20th International Symposium on Ballistics,2002

[3] Rabern D.A : Axially Accelerated Saboted Rods Subjected to Lateral Forces; LANL report LA-11494-MS; 1989.

[4] Wilkerson S., Hopkins D.: Analysis of a Balanced Breech System for the M1A1 Main Gun System Using Finite Element Techniques; ARL Report ARL-TR-608; 11/1994.

[5] Wilkerson S., Hopkins D., Held B. : Techniques for Modelling Bullet Exit Conditions Predicted by Transient Finite Element Models; 8th Symposium on gun dynamics; 1996.
[6] Eches N., Paugain N., Sabourin P., Boisson D., Barthelemy F. : Influence of the rifling geometry on the interaction between an artillery gun and an ammunition; 17th International Symposium on Ballistics, 1998